Supporting Information

Self-Templated Formation of $(NiCo)_9S_8$ Yolk-Shelled Spheres for High Performance Hybrid Supercapacitors

Yi-Lin Liu[a,b,1], Cheng Yan[a,c,1], Gui-Gen Wang[a,*], Fei Li[a], Yang Shang[b], Hua-Yu Zhang[a], Jie-Cai Han[a,c], Hui Ying Yang[b,*]

[a]*Shenzhen Key Laboratory for Advanced Materials, Harbin Institute of Technology, Shenzhen, Shenzhen 518055, P. R. China*
wangguigen@hit.edu.cn (Gui-Gen Wang)
[b]*Pillar of Engineering Product Development, Singapore University of Technology and Design, 8 Somapah Road, Singapore 487372, Singapore*
yanghuiying@sutd.edu.sg (Hui Ying Yang)
[c]*School of Chemistry, Faculty of Science, The University of Sydney, Sydney 2006, Australia*
[d]*National Key Laboratory of Science and Technology on Advanced Composites in Special Environments, Harbin Institute of Technology, Harbin 150080, China*

[1] Y.L.L. and C.Y. contributed equally to this work.

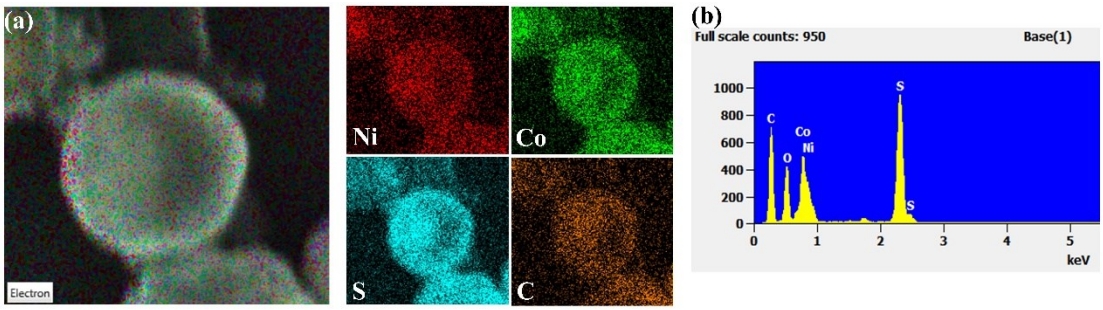

Figure S1. $(NiCo)_9S_8$/C-600 sphere (a) elemental mapping of Ni, Co S and C, (b) EDS.

Spectrum. respectively.

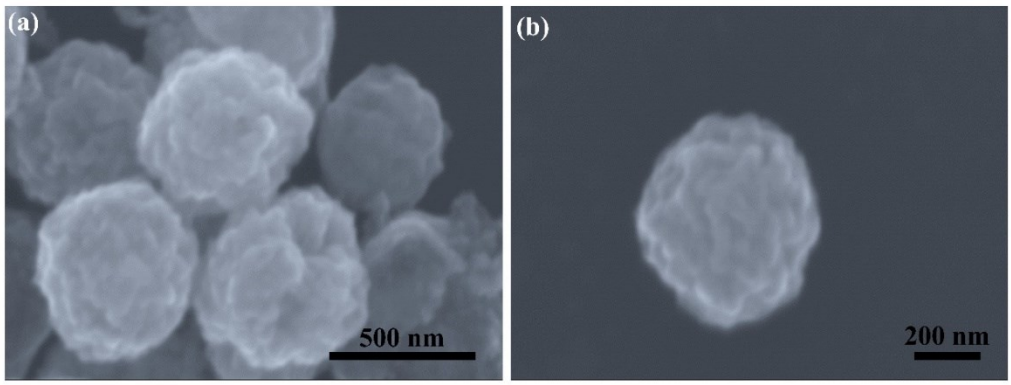

Figure S2. SEM images of $(NiCo)_9S_8$/GC-400: (a) Low magnification; (b) High magnification.

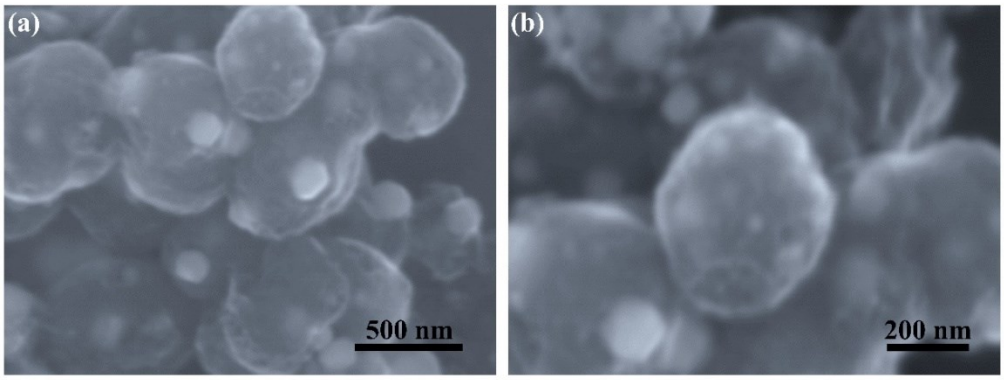

Figure S3. SEM images of $(NiCo)_9S_8$/GC-800: (a) Low magnification; (b) High magnification.

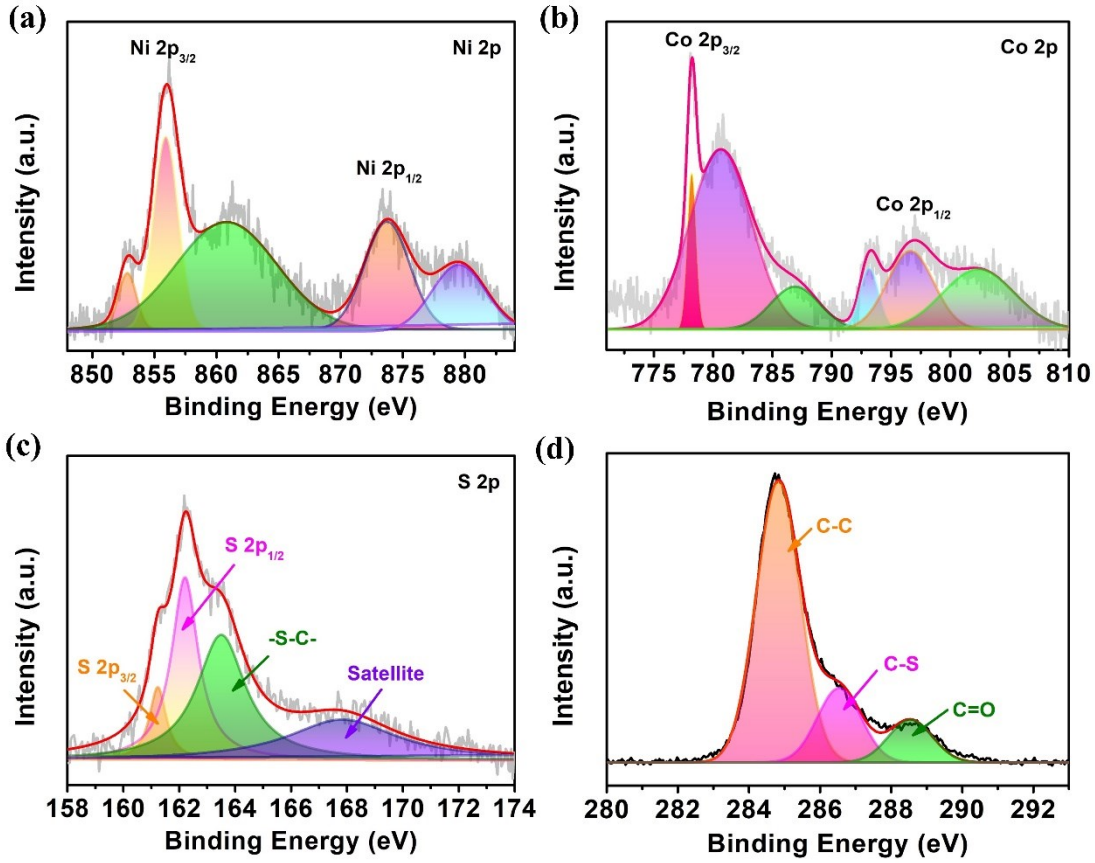

Figure S4. XPS spectra of the as-obtained $(NiCo)_9S_8$/GC-400 spheres: (a) Ni 2p; (b) Co 2p; (c) S 2p and (d) C 1s.

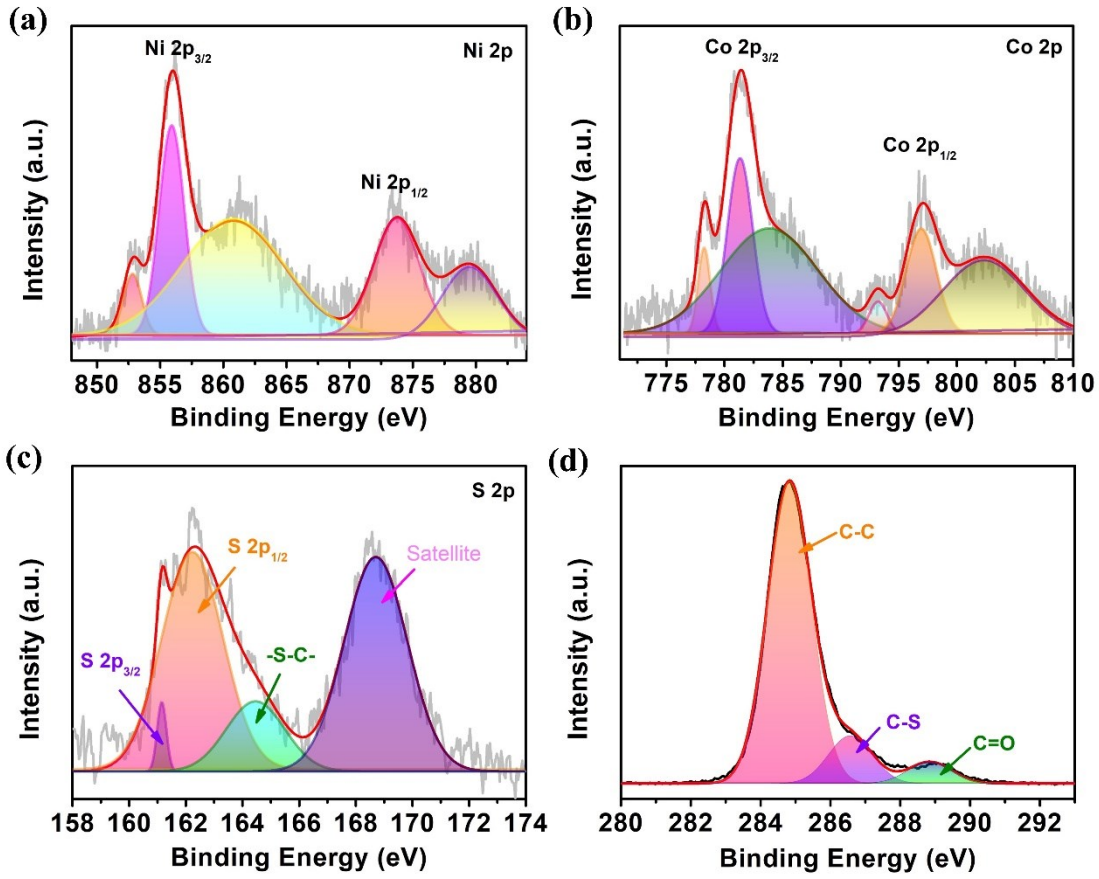

Figure S5. XPS spectra of the as-obtained $(NiCo)_9S_8$/GC-800 spheres: (a) Ni 2p; (b) Co 2p; (c) S 2p and (d) C 1s.

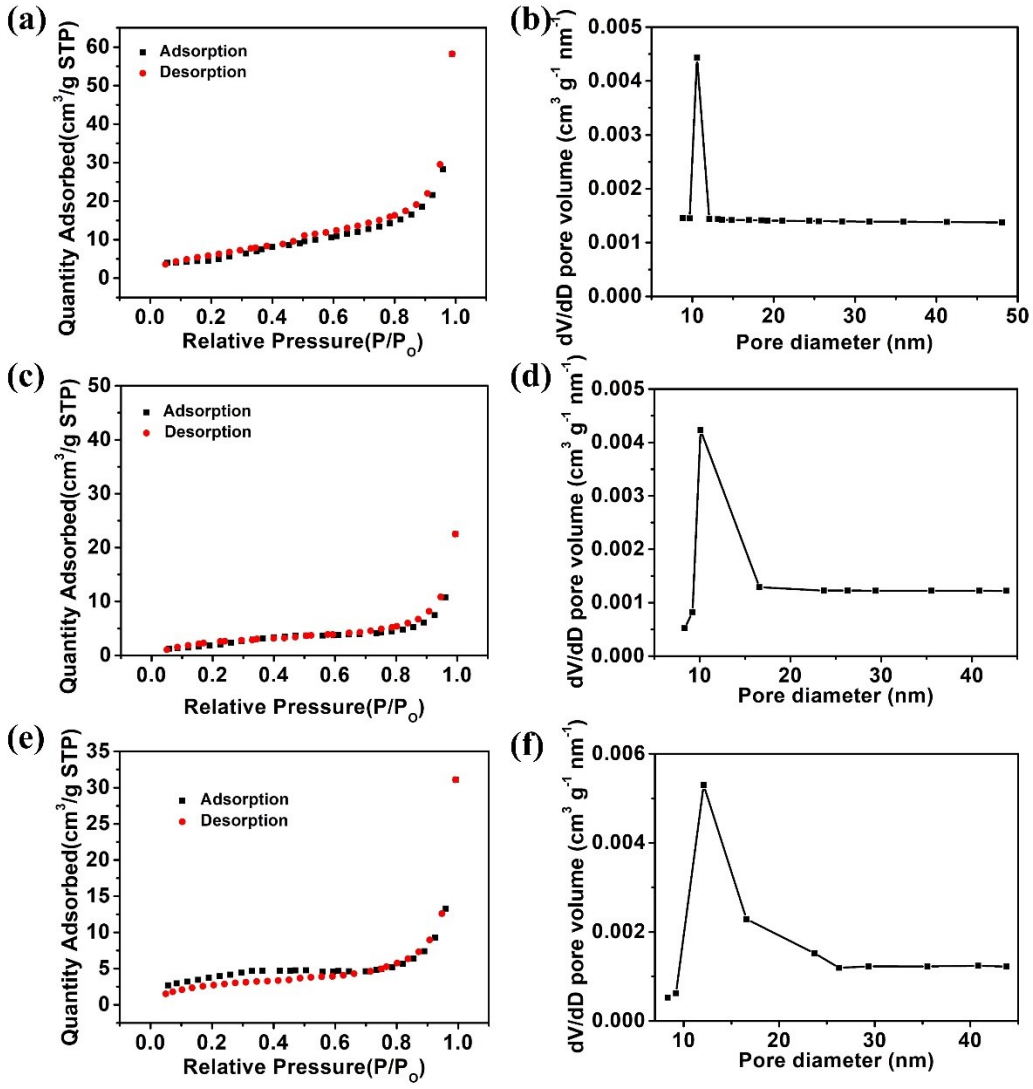

Figure S6. BET measurements: Nitrogen adsorption/desorption isotherms and the pore-size distribution. a-b) $(NiCo)_9S_8$/GC-400; c-d) $(NiCo)_9S_8$/GC-600; e-f) $(NiCo)_9S_8$/GC-800.

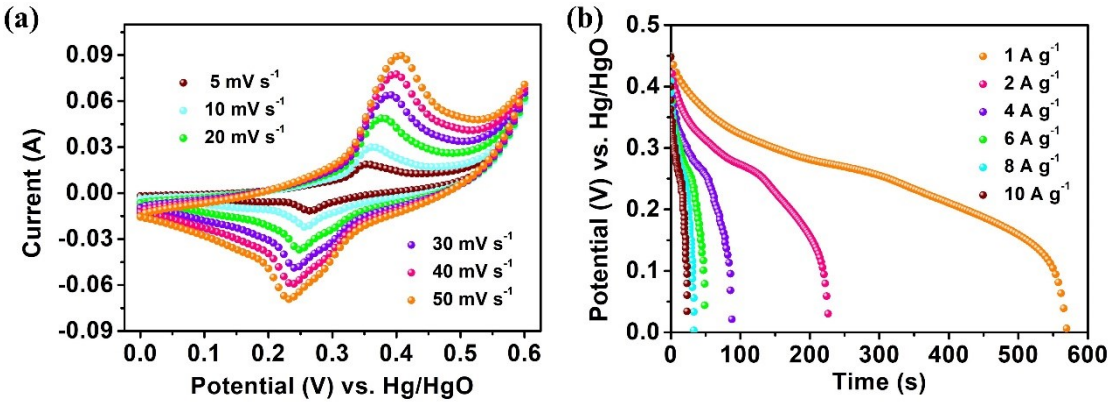

Figure S7. The electrochemical performance of the $(NiCo)_9S_8$/GC-400 spheres: (a) The CV curves; (b) The discharge curves.

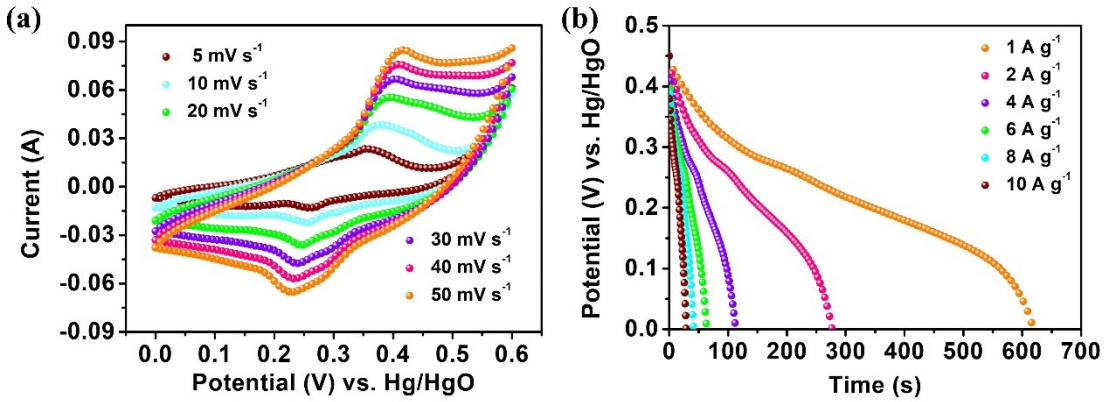

Figure S8. The electrochemical performance of the $(NiCo)_9S_8$/GC-800 spheres: (a) The CV curves; (b) The discharge curves.

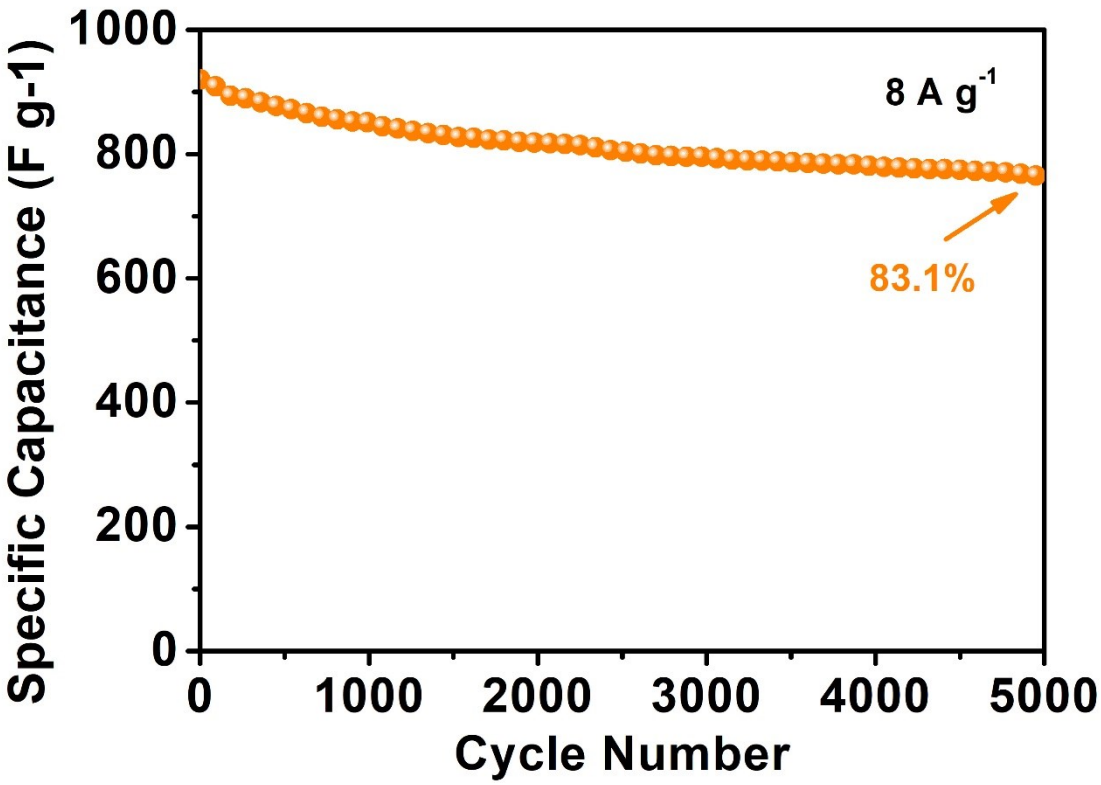

Figure S9. The cycling performance of the yolk-shelled $(NiCo)_9S_8$/GC-600 sphere.

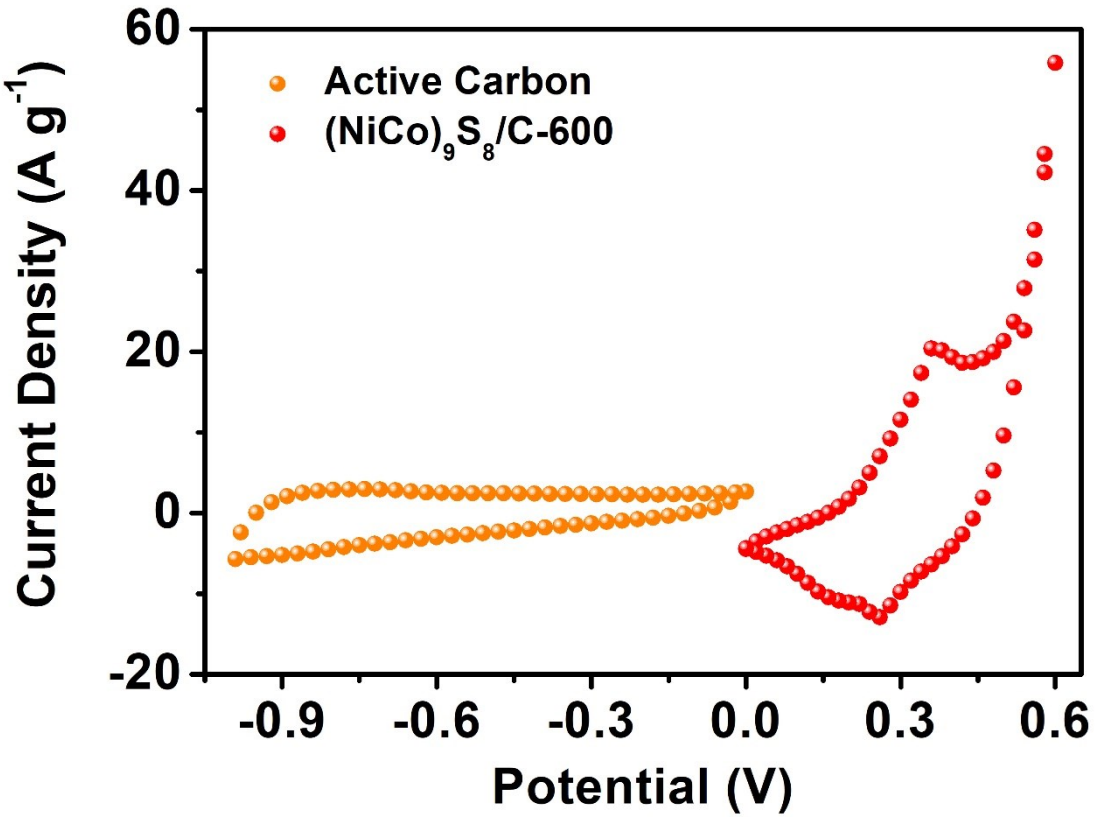

Figure S10. CV curves of AC and yolk-shelled $(NiCo)_9S_8$/GC-600 sphere at the scan rate of 5 mV s^{-1}.

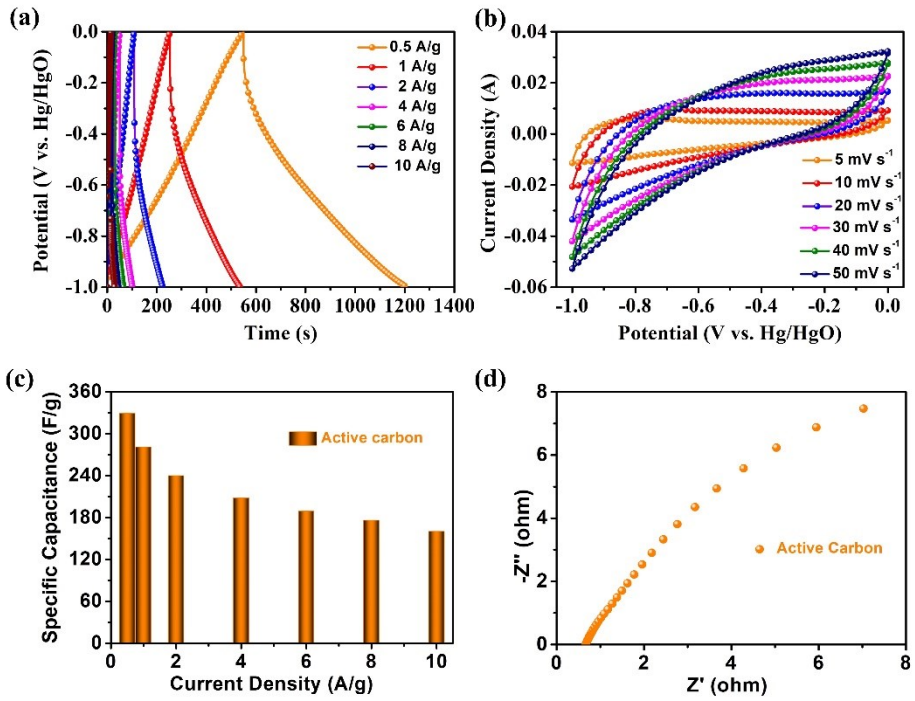

Figure S11. The electrochemical performance of AC: (a) The CV curves; (b) The GCD curves; (c) Rate performance; (d) EIS curves.

Table S1. Comparison of electrochemical performance between various hybrid pseudocapacitive electrodes and our work.

Electrode composition	Electrolyte	Specific capacitance	Counter electrode	Cyclic stability	Ref.
$(NiCo)_9S_8$	2M KOH	1434.4 F g^{-1} at 1 A g^{-1}/	Hg/HgO electrode	83.1 % after 5000 cycles	This work
$NiCo_2S_4$ Nanoflakes[1]	2M KOH	908.1 F g^{-1} at 1 A g^{-1}	saturated calomel electrode	87.7 % after 2000 cycles	S1
Porous $NiCo_2S_4$[2]	6M KOH	1268 F g^{-1} at 1 A g^{-1}	Ag/AgCl electrode	82 % after 10000 cycles	S2
$NiCo_2S_4$ Nanosheets[3]	1M KOH	1394.5 F g^{-1} at 1 A g^{-1}	Ag/AgCl electrode	124 % after 10000 cycles	S3
$NiCo_2S_4$ nanoparticles[4]	6M KOH	1090 F g^{-1} at 2 A g^{-1}	Hg/HgO electrode	80.1 % after 3000 cycles	S4
$NiCo_2S_4$ nanorod[5]	1M KOH	1130 F g^{-1} at 0.4 A g^{-1}	Hg/HgO electrode	80 % after 1000 cycles	S5
$NiCo_2S_4$ nanotubes[6]	1M KOH	1240 F g^{-1} at 1 A g^{-1}	Hg/HgO electrode	80 % after 5000 cycles	S6
Co_9S_8/S-rGO[7]	6M KOH	708.3 F g^{-1} at 1 A g^{-1}	Hg/HgO electrode	71.2 % after 2000 cycles	S7
Co_9S_8/GO[8]	6M KOH	540 C g^{-1} at 4 A g^{-1}	Hg/HgO electrode	93.9 % after 1000 cycles	S8
$CoNi_2S_4/Co_9S_8$[9]	3M KOH	1183.3 F g^{-1} at 2 A g^{-1}	Ag/AgCl electrode	98.1 % after 1000 cycles	S9

Co_9S_8[10]	1M KOH	514 F g^{-1} at 1 A g^{-1}	Ag/AgCl electrode	88 % after 1000 cycles	S10

References

[1] Y. Zheng, J. Xu, X. Yang, Y. Zhang, Y. Shang, X. Hu, Decoration $NiCo_2S_4$ nanoflakes onto ppy nanotubes as core-shell heterostructure material for high-performance asymmetric supercapacitor, Chem. Eng. J. 333 (2018) 111-121.

[2] Q. Gao, X. Wang, Z. Shi, Z. Ye, W. Wang, N. Zhang, Z. Hong, M. Zhi, Synthesis of porous $NiCo_2S_4$ aerogel for supercapacitor electrode and oxygen evolution reaction electrocatalyst, Chem. Eng. J. 331 (2018) 185-193.

[3] Y. Liu, Z. Li, L. Yao, S. Chen, P. Zhang, L. Deng, Confined growth of $NiCo_2S_4$ nanosheets on carbon flakes derived from eggplant with enhanced performance for asymmetric supercapacitors, Chem. Eng. J. 366 (2019) 550-559.

[4] Y. Zheng, X. Wang, W. Zhao, X. Cao, J. Liu, Phytic acid-assisted synthesis of ultrafine $NiCo_2S_4$ nanoparticles immobilized on reduced graphene oxide as high-performance electrode for hybrid supercapacitors, Chem. Eng. J. 333 (2018) 603-612.

[5] B. Li, B. Luo, J. Zhao, Y. Pan, H. Zhou, Y. Xiao, S. Lei, B. Cheng, high electrical conductivity-induced enhancement effect of electrochemical performance in mesoporous $NiCo_2S_4$ nanorod-based supercapacitor, J. Energy Storage 26 (2019) 100955.

[6] Y. Chen, T. Liu, L. Zhang, J. Yu, $NiCo_2S_4$ Nanotubes Anchored 3D nitrogen-doped graphene framework as electrode material with enhanced performance for asymmetric supercapacitors, ACS Sustain. Chem. Eng. 7 (2019) 11157-11165.

[7] Y. Yang, F. Ma, J. Wang, J. Li, J. Cao, W. Han, H. Gu, Y. Zhang, Comparative analysis of Co_9S_8/S-doped rGO composites as high-performance electrodes via facile one-step anneal fabrication for supercapacitor application, J.Alloy. Compd. 815 (2020) 152448.

[8] B. Xie, M. Yu, L. Lu, H. Feng, Y. Yang, Y. Chen, H. Cui, R. Xiao, J. Liu, Pseudocapacitive Co_9S_8/graphene electrode for high-rate hybrid supercapacitors, Carbon 141 (2019) 134-142.

[9] F. Zhao, W. Huang, H. Zhang, D. Zhou, Facile synthesis of $CoNi_2S_4$/Co_9S_8 composites as advanced electrode materials for supercapacitors, Appl. Surf. Sci. 426 (2017) 1206-1212.

[10] T.-W. Lin, H.-C. Tsai, T.-Y. Chen, L.-D. Shao, Facile and controllable one-pot synthesis of hierarchical Co_9S_8 hollow microspheres as high-performance electroactive materials for energy storage and conversion, ChemElectroChem 5 (2018) 137-143.